AIP | Journal of Applied Physics

The effect of thermal anisotropies during crystallization in phase-change recording media

M. R. Belmont, M. M. Aziz, and C. D. Wright

Citation: J. Appl. Phys. **104**, 044901 (2008); doi: 10.1063/1.2968447
View online: http://dx.doi.org/10.1063/1.2968447
View Table of Contents: http://jap.aip.org/resource/1/JAPIAU/v104/i4
Published by the American Institute of Physics.

The effect of thermal anisotropies during crystallization in phase-change recording media

M. R. Belmont, M. M. Aziz,[a] and C. D. Wright
School of Engineering, Computer Science and Mathematics, University of Exeter, Harrison Building, North Park Road, Exeter EX4 4QF, United Kingdom

(Received 11 April 2008; accepted 13 June 2008; published online 20 August 2008)

The problem discussed is the significance of anisotropies in the thermal parameters of different phases of phase-change materials as used for data storage purposes during recording. The particular phase change in interest is from the amorphous-to-crystalline state. Applying the method of correlation moment analysis produced upper estimators for the time dependence of the width of the crystalline mark and the time at which phase change ceases based on the heat flow process alone. These upper estimators are closed-form analytical expressions that can be used to estimate the recording resolution for any general spatial profile of initial temperature in the medium. This analysis showed that, up to a first order, the specific heat anisotropies have considerably less influence on the heat flow than the thermal conductivity differences. In general, for the material parameters used in phase-change data storage applications, the theory showed that the anisotropy in thermal parameters can be neglected. © *2008 American Institute of Physics*.
[DOI: 10.1063/1.2968447]

I. INTRODUCTION

A key property of data storage media is the minimum size scale over which information-bearing structures can be produced and read. In certain classes of materials these structures are based on the different properties of crystalline and amorphous phases.[1,2] Consequently the pattern of these structures and hence the storage density are controlled by the spatial profile of the temperature and its time evolution used to induce the phase transition. The determination of this temperature profile is hampered by a combination of (i) the inherently anisotropic characteristics of materials with two such phases present and (ii) the nonlinear nature of the thermal processes and the kinetics of the phase transition.[3,4]

The nonlinearity has a further effect in that unlike linear problems, where only parametric variations occur, in nonlinear processes the actual character of the solutions for temperature and thus phase composition will vary with the initial conditions. Thus, recording resolution will vary with both (i) the spatial data pattern desired to be written and hence the impressed temperature profile and (ii) the initial concentration profiles of the two phases. A major consequence of this is that numerical explorations can become very intensive as it is not possible to explore parametric effects of the material properties without exhaustive evaluations over large classes of initial conditions. An analytic approach that provides even indirect information on the role of the anisotropies in material parameters and recording resolution is clearly of value.

The main goal here is not to secure precise values for resolution limits in individual cases, which is more the province of highly specific numerical solutions, but to identify the manner and degree in which the differences in properties between phases affect the phase-change process itself and as a consequence their role in determining the achievable recording resolution in general. A key practical outcome of the present work is an assessment of the errors involved in the commonly used assumption of isotropic linear heat flow and the way these errors depend on the various anisotropies. The class of mark patterns to be explored here is deterministic dealing with individual marks and is aimed at yielding information about factors affecting the limits of resolution.

The form of the kinetic equation that is used in this work makes a direct solution approach unrealistic. As a result, the analysis presented here involves exploring the heat flow equation in the presence of the phase change but without the detail of the kinetic mechanism. Using the correlation moment technique,[5] an approximation for the time dependence of a measure of the width of the crystalline region will be produced. The results of this analysis make it possible to determine which are the dominant anisotropy parameters and how they affect the width measure. In addition, it allows estimation of the time at which thermal spreading stops and hence the expected final crystalline mark widths. However, this analysis is based on the heat diffusion process alone and hence provides upper estimates for the spreading time and length scales in this problem. The detailed kinetics are included in another report[6] by examining the role of the initial peak temperature, and hence energy density in the medium, and considering the relative contributions to the crystallization rate made by the thermal diffusive flow and the phase-change reaction rate.

The fundamental equations of the heat diffusion process and reaction rate are presented in Sec. II of this paper, and nondimensionalized to simplify the analysis and to identify the nonlinear contributions to the problem. Section III describes briefly the correlation moment technique and relevant moments to obtain upper estimates for the time dependent width measures of the crystalline mark. Moreover, this section also uses correlation moment properties to arrive at upper estimates for the time when phase change ceases and the expected final mark widths.

[a]Electronic mail: m.m.aziz@ex.ac.uk.

It is important to note that this work focuses on the effects of thermal anisotropies and kinetics on the intrinsic material properties and length scales, and no attempt is made to include the influences of thermal and heat sinking layers on these properties and length scales. These effects are discussed in more detail elsewhere.[7–9] Moreover, the treatment of kinetics here does not account for incubation times for the onset of crystallization and hence applies more to melt quenched or primed[10] amorphous phase-change media.

II. FUNDAMENTAL EQUATIONS

A. The reaction rate equation

The reaction rate for volume fraction conversion from amorphous-to-crystalline phases will be described by the Arrhenius relationship[11]

$$\frac{\partial \chi(x,t)}{\partial t} = (1-\chi(x,t))A_c \exp\left(\frac{-E_c}{kT(x,t)}\right), \tag{1}$$

where the pre-exponential frequency term A_c and activation energy for crystallization E_c are temperature independent, k is Boltzmann's constant, and T is absolute temperature. The fraction $\chi(x,t)$ is the microscale volume fraction of the crystalline phase. To minimize the complexity of the analysis, it is assumed here that the reverse reaction rate from crystalline to amorphous is negligible.

B. Heat balance equation

The microscale, one-dimensional heat balance equation is

$$\rho_o \frac{\partial C\{\chi(x,t)\}T(x,t)}{\partial t} + \rho_o \frac{\partial L\{\chi(x,t)\}}{\partial t} = \frac{\partial}{\partial x}\left(K\{\chi(x,t)\}\frac{\partial T(x,t)}{\partial x}\right), \tag{2}$$

where $C\{\chi(x,t)\}$ and $K\{\chi(x,t)\}$ are the microscale, time dependent values of the specific heats and thermal conductivities for the two phases and $L\{\chi(x,t)\}$ is the latent heat for the phase transition. The change in volume associated with the phase transition is normally small[12,13] ($\sim$6% for $Ge_2Sb_2Te_5$) and considered here as negligible to reduce the mathematical complexity of the analysis. Hence the average density between the amorphous and crystalline phases ρ_o is used in Eq. (2). Given a standard multisite model nucleation process,[14] it is possible to invoke local average properties where

$$C\{\chi(x,t)\} = C_c\langle\chi(x,t)\rangle + C_a\langle 1-\chi(x,t)\rangle,$$

$$K\{\chi(x,t)\} = K_c\langle\chi(x,t)\rangle + K_a\langle 1-\chi(x,t)\rangle,$$

and

$$L\{\chi(x,t)\} = L_c\langle\chi(x,t)\rangle,$$

in which the isotropic specific heats C_c and C_a and the isotropic thermal conductivities K_c and K_a of the crystalline and amorphous phases, respectively, are considered to be temperature independent. A similar assumption is made about the isotropic latent heat of crystallization L_c. $\langle\chi(x,t)\rangle$ is the macroscale average of the microscale crystalline volume fraction $\chi(x,t)$. This description of the microscale averaged thermal properties is legitimate providing that $|\partial\chi(x,t)/\partial x| \gg |\partial T(x,t)/\partial x|$, i.e., the length scales of the macroscopic quantities such as the temperature are substantially larger than those of the local nucleites, which is usually the case in data storage applications.

In terms of the averaged quantities, Eq. (2) after manipulation becomes

$$\frac{\partial T(x,t)}{\partial t} + \frac{(C_c-C_a)}{C_a}\frac{\partial\langle\chi(x,t)\rangle T(x,t)}{\partial t} + \frac{L_c}{C_a}\frac{\partial\langle\chi(x,t)\rangle}{\partial t} = \frac{K_a}{\rho_o C_a}\frac{\partial^2 T(x,t)}{\partial x^2} + \frac{(K_c-K_a)}{\rho_o C_a}\frac{\partial}{\partial x}\left(\langle\chi(x,t)\rangle\frac{\partial T(x,t)}{\partial x}\right). \tag{3}$$

For compactness the $\langle\ \rangle$ symbols will be dropped, and henceforth it is to be understood that the notation refers to macroscopic average values.

C. The heat source

Equation (3) does not contain explicit heat source terms, and thus the heat energy for initiating the phase transition enters via the initial conditions. This choice is made for technical reasons associated with correlation moment analysis that will be used subsequently. Physically the present situation corresponds to a fast heating source with a delta function temporal profile having zero rise, fall times, and duration. This means that the amorphous-to-crystalline phase transition will take place during cooling rather than heating. Such an approach is of interest commercially as a route to substantial increases in writing/erasing speeds[15] and is analyzed further in the second stage of the analysis.[6]

D. Nondimensionalizing the heat balance and kinetic equations

The independent variables x and t together with the dependent variable $T(x,t)$ can be rescaled to produce a normalized equation system whose coefficients allow assessment of the relative significance of the respective terms. The scaling relationships used are $x=x_o\eta$, $t=t_o\tau$, and $T(x,t)-T_o=T_o\psi(\eta,\tau)$, where x_o and t_o are the size scales of the variables in the problem and T_o is the ambient temperature. The volume fraction of the crystalline material χ does not require rescaling.

Substituting the rescaled variables and setting $K_a t_o/(x_o^2 C_a \rho_o)=1$ results in a nondimensionalized form of the heat balance equation where the linear terms have coefficients of unity and the nonlinear terms are scaled by $\varepsilon_1=(C_c-C_a)/C_a$, $\varepsilon_2=L_c/(C_a T_o)$, and $\varepsilon_3=(K_c-K_a)/K_a$, respectively, i.e., Eq. (3) becomes

$$\frac{\partial\Psi(\eta,\tau)}{\partial\tau} + \varepsilon_1\frac{\partial\chi(\eta,\tau)\Psi(\eta,\tau)}{\partial\tau} + (\varepsilon_1+\varepsilon_2)\frac{\partial\chi(\eta,\tau)}{\partial\tau} = \frac{\partial^2\Psi(\eta,\tau)}{\partial\eta^2} + \varepsilon_3\frac{\partial}{\partial\eta}\left(\chi(\eta,\tau)\frac{\partial\Psi(\eta,\tau)}{\partial\eta}\right). \tag{4}$$

Substituting the scaling relationships into the kinetics, Eq. (1) results in the nondimensionalized form

TABLE I. List of thermal, kinetic, and structural parameters for $Ge_2Sb_2Te_5$ available from literature and used throughout this work. ρ_o is the average density of the material, T_m and T_c are the melting and crystallization temperature of the material, L_c is the latent heat of crystallization, C and K are the specific heat and thermal conductivity of the material, respectively (subscript a, amorphous phase and subscript c, crystalline phase), and α is the thermal diffusivity of the amorphous phase. E_c is the activation energy for crystallization, and A_c is the frequency term.

Symbol	Value	Units
ρ_o	5995[a]	kg/m^3
T_m (5 K/min)	894[b]	K
T_c (80 K/min)	446[b]	K
L_c	3.9[b,c]	kJ/kg
C_a	218[d]	J/(kg K)
C_c	563[e]	J/(kg K)
K_a (300 K)	0.23[f,g]	W/(m K)
K_c (464 K)	0.3[g,h]	W/(m K)
$\alpha=K_a/(r_oC_a)$	176×10^{-9}	m^2/s
E_c	2.24[i,j,k]	eV
A_c	1.5×10^{22} [j]	s^{-1}

[a]Reference 12.
[b]Reference 16.
[c]Reference 17.
[d]Dulong–Petit value for the molar heat capacity at constant pressure; i.e., $C=3$ Nk for nine atoms of $Ge_2Sb_2Te_5$ also appeared in Refs. 1 and 2.
[e]Reference 18.
[f]Reference 19.
[g]Reference 20.
[h]Reference 21. This value is lower than the published value in Ref. 19 at room temperature (0.53 W/m K) and reflects the thermal conductivity value at elevated temperatures and near the transition point (metastable state), which is more relevant to this work.
[i]Reference 3.
[j]Reference 4.
[k]Reference 22.

$$\frac{\partial\chi(\eta,\tau)}{\partial\tau}=[1-\chi(\eta,\tau)]\Delta\exp\left[\frac{-\gamma}{\Psi(\eta,\tau)+1}\right], \tag{5}$$

where $\Delta=t_oA_c$ and $\gamma=E_c/(kT_o)$.

The nondimensionalized heat balance in Eq. (4) contains both isotropic linear terms and anisotropic nonlinear contributions. The degree of nonlinearity is determined by the magnitudes of the factors $\varepsilon_1\rightarrow\varepsilon_3$, which measure the extent of the departure from isotropic behavior. In this sense the heat flow is a perturbed linear system. In contrast the typically large values of the factor $\gamma=E_c/(kT_o)$ (due to the large activation energy of materials used in data storage) in the kinetic equation mean that under conditions where heat flow is still very close to linear the kinetics can be strongly nonlinear.

Examining ε_2, the coefficient of the latent heat term shows that it defines the ratio of the latent heat L_c to the stored heat C_aT_o. Using the appropriate parameter values found in literature for the materials of interest as listed in Table I, the latent heat term coefficient $\varepsilon_2\sim0.05$. Thus if it is useful to do so the latent heat term can be neglected, which is typically the assumption made in the literature. However as is shown in Eq. (4), the latent heat coefficient ε_2 can be conveniently grouped with the specific heat coefficient ε_1, and hence there is no advantage in dropping the latent heat contribution.

III. CORRELATION MOMENT ANALYSIS

This part of the analysis develops an estimate for the time dependence of the measure of the crystalline phase width during cooling from the initial condition but without detailed kinetics using the correlation moment technique.[5] The power of the method is that it generates these measures directly from the defining equations without the need to explicitly solve them, and since, as in the present case, these defining equations are often analytically intractable nonlinear partial differential equations, this is a valuable attribute.

The autocorrelation function $R(\lambda)$ can be used as a descriptor for the spatial characteristics of quantities such as the profiles of the temperature T and the fraction of the crystalline phase χ in data recording studies. Four reasons why $R(\lambda)$ is attractive are as follows: (i) a given autocorrelation function can characterize a broad class of spatial data patterns with the resolution being associated with the various moments of $R(\lambda)$, (ii) the width of the main lobe of $R(\lambda)$ can be a sensitive measure of spatial resolution, and (iii) is equally well defined for deterministic and stochastic situations. This third reason is particularly useful in the present case that focuses on local mark properties. These have relatively symmetrical pulselike spatial profiles, and the method exploits the well-known characteristics of the autocorrelation for such functions.[23] Finally, (iv) correlation functions are integral measures taken over the whole domain; consequently it is possible to assess the relative contribution of various terms even when they are locally very stiff (during the fast kinetics regime the phase-change region is very similar to an internal boundary layer). This is particularly useful because in typical data storage materials the factor $\gamma=E_c/(kT_o)$ in the exponent of the rate equation can be substantial, leading to very large partial and temporal $\chi(x,t)$ derivatives over localized regions. The physical interpretation of this is the well-known phenomenon in data storage work—that annealing can take place rapidly over narrow regions.[24] Such behavior is reminiscent of free boundary layers in fluid mechanics or flamelet structures in combustion analysis and makes it very difficult to invoke global statements about the relative significance of terms in, for example, Eq. (4). However because correlation moments are integral metrics evaluated over the whole domain, thus avoiding such local problems allows sensible assessments to be made from the respective scale of terms. For deterministic functions, correlation moments measure the distribution of some quantity in an analogous sense to the moment of inertia of a mass distribution. As with all such metrics this will be a function of the spatial distribution of the quantity of interest.

The key quantity of interest in the correlation moment analysis, for the case under investigation, is the time dependent second moment $\Gamma_{f_1,f_1,2}(t)$ of the spatial autocorrelation function $R_{f_1,f_1}(\lambda,t)$ of the quantity $f_1(x,t)$, where

$$\Gamma_{f_1,f_1,2}(t)=\int_{-\infty}^{\infty}\lambda^2R_{f_1,f_1}(\lambda,t)d\lambda. \tag{6}$$

Similarly, moments can be defined for cross correlation functions. For two functions $f_1(x,t)$ and $f_2(x,t)$, which are both

$\in L^2\Re$, it is readily shown that the r^{th} moment $\Gamma_{f_1,f_2,r}(t)$ is given by[5]

$$\Gamma_{f_1,f_2,r}(t) = \int_{-\infty}^{\infty}\int_{-\infty}^{\infty}(\zeta-\nu)^r f_1(\zeta,t)f_2(\nu,t)d\nu d\zeta. \tag{7}$$

Appropriately normalizing $\Gamma_{f_1,f_1,2}(t)$ produces a measure of the mean square width $\lambda_w^2(t)$ of $R_{f_1,f_1}(\lambda,t)$. The simplest normalizing quantity, which is appropriate for the length scales of the order of individual marks in this work,[5] is $\Gamma_{f_1,f_1,0}(t)$; and thus

$$\lambda_w^2(t) = \left|\frac{\Gamma_{f_1,f_1,2}(t)}{\Gamma_{f_1,f_1,0}(t)}\right|. \tag{8}$$

This is especially useful where the quantities of interest are conserved for then $\Gamma_{f_1,f_1,0}(t)$ is time independent.

The definition of correlation used in correlation moment analysis[5] means that the quantities of interest such as $\chi(x,t)$ and $T(x,t)$ must $\in L^2\Re$; hence they must have the property

$$\int_{-\infty}^{\infty}|\chi(x,t)|^2|T(x,t)|^2dx < M, \tag{9}$$

where M is a bounded positive real number. For positive quantities such as $\chi(x,t)$ and $T(x,t)$, this results in the additional requirement that

$$\int_{-\infty}^{\infty}\frac{\chi(x,t)}{T(x,t)}dx < M, \tag{10}$$

i.e., $\chi(x,t)$ and $T(x,t)$ are both $\in L\Re$.

While this behavior is typically true for $\chi(x,t)$ it is not the case for $T(x,t)$ because $\lim_{|x|\to\infty}T(x,t)\to T_o$, where T_o is the ambient temperature. However the choice of $\psi=(T-T_o)/T_o$ was deliberately made to ensure that the normalized temperature has the required characteristics that $\lim_{|\eta|\to\infty}T(\eta,\tau)\to 0$. Thus the variables in Eq. (4) have all the attributes needed to legitimize the use of correlation moment analysis.

The first step is to transform Eq. (4) into an ordinary differential equation in terms of $\Gamma_{\psi,\psi,2}(\tau)$ with τ as the independent time variable. This entails the use of a premultiplier of the form $\psi(\eta+\lambda,\tau)+\psi(\eta-\lambda,\tau)$, where λ is the spatial correlation lag variable. By using this premultiplier together with various properties of correlation moments[5] it can be shown that Eq. (4) transforms to

$$\begin{aligned}&\frac{d\Gamma_{\Psi,\Psi,r}(\tau)}{d\tau}+\varepsilon_1\left[\frac{d\Gamma_{\chi+\Psi,\Psi,r}(\tau)}{d\tau}+\frac{d\Gamma_{\chi-\Psi,\Psi,r}(\tau)}{d\tau}\right.\\&\left.-4\Gamma_{\chi\Psi,\Psi,r-2}(\tau)+O(\varepsilon)\right]+(\varepsilon_1+\varepsilon_2)\left[\frac{d\Gamma_{\Psi,\Psi,r}(\tau)}{d\tau}\right.\\&\left.+\frac{d\Gamma_{\Psi,\Psi,r}(\tau)}{d\tau}-4\Gamma_{\Psi,\chi,r-2}(\tau)+O(\varepsilon)\right]\\&=4\Gamma_{\Psi,\Psi,r-2}(\tau)+\varepsilon_3 4\Gamma_{\Psi,\chi(\partial\Psi/\partial\eta),r-1}(\tau),\end{aligned} \tag{11}$$

where $O(\varepsilon)$ denotes terms with coefficients that are order 1 or higher in ε_1, ε_2, or ε_3. Terms with coefficients of order greater than 1 will be ignored in this first order analysis.

A. Time dependence of the width of the crystalline fraction

The correlation moment that defines the width of the crystalline phase at a given time is $\Gamma_{\chi,\chi,2}(\tau)$. As previously indicated the form of the kinetics equation makes this inaccessible directly; however, it is possible to obtain an upper estimate for $\Gamma_{\chi,\chi,2}(\tau)$ from the heat flow correlation moment equation alone, without explicit inclusion of Eq. (5) as discussed next.

After application of the initial temperature profile, the region over which the phase transition occurs is initially very narrow. Then the crystalline fraction $\chi(\eta,\tau)$ is approximately a unity amplitude Heaviside pulse function. Consequently $\chi(\eta,\tau)$ is initially a unity amplitude window function for $\Psi(\eta,\tau)$ that follows the diffusive thermal spreading (when this behavior ceases to be the case it will be shown that the spreading of the crystalline region will be over on practical time scales). One effect of this is that the sequence of spatial correlation functions $R_{\Psi,\Psi}(\lambda,\tau)$, $R_{\chi\Psi,\Psi}(\lambda,\tau)$, $R_{\Psi,\chi}(\lambda,\tau)$, and $R_{\chi\Psi,\Psi}(\lambda,\tau)$ exhibits similar general forms and has reducing relative width. Given that the $r=2$ correlation moments for this class of function are positive, then the $r=2$ correlation moments and the magnitudes of the associated temporal derivatives of $R_{\chi\chi}(\lambda,\tau)$, $R_{\Psi,\chi}(\lambda,\tau)$, and $R_{\chi\Psi,\Psi}(\lambda,\tau)$ will be somewhat less than that of $R_{\Psi,\Psi}(\lambda,\tau)$.

This result means that $d\Gamma_{\Psi,\Psi,r}(\tau)/d\tau$ can be used as an upper estimator for all members of the sequence of positive growth rates $d\Gamma_{\chi\Psi,\Psi,r}(\tau)/d\tau$, $d\Gamma_{\Psi,\chi,r}(\tau)/d\tau$, and of particular relevance $d\Gamma_{\chi,\chi,r}(\tau)/d\tau$. Similarly $\Gamma_{\Psi,\Psi,r}(\tau)$ is an upper estimator for $\Gamma_{\chi\Psi,\Psi,r}(\tau)$ and $\Gamma_{\Psi,\chi,r}(\tau)$ with $\Gamma_{\Psi,\partial\Psi/\partial\eta,r}(\tau)$. Equally, the function serves the same role for $\Gamma_{\Psi,\partial\Psi/\partial\eta,r}(\tau)$.

Using these upper estimator quantities in Eq. (11) and omitting second order terms in ε produces the following relationship for $\Gamma_{\Psi,\Psi,2}(\tau)$ and hence the upper bound to $\Gamma_{\chi,\chi,2}(\tau)$ as denoted by $\Gamma^{\text{upper}}_{\chi,\chi,2}(\tau)$:

$$\frac{d\Gamma^{\text{upper}}_{\chi,\chi,2}(\tau)}{d\tau}[1+2\varepsilon_1+\varepsilon_2]\approx 4\Gamma_{\Psi,\Psi,0}(\tau)[1+2\varepsilon_1+\varepsilon_2+\varepsilon_3], \tag{12}$$

where use has been made of the correlation moment property[5] $\Gamma_{\Psi,\partial\Psi/\partial\eta,1}(\tau)=\Gamma_{\Psi,\Psi,0}(\tau)$.

Now Eq. (7) readily shows that $\Gamma_{\Psi,\Psi,0}(\tau)=\int_{-\infty}^{\infty}\Psi(\eta,\tau)^2d\eta$, which is a conserved quantity and hence $\Gamma_{\Psi,\Psi,0}(\tau)=\Gamma_{\Psi,\Psi,0}(0)$. Using the above results, Eq. (12) integrates to

$$\Gamma^{\text{upper}}_{\chi,\chi,2}(\tau) = 4\beta\tau\Gamma_{\Psi,\Psi,0}(0)+\Gamma^{\text{upper}}_{\chi,\chi,2}(0), \tag{13}$$

where

$$\beta = \frac{1+2\varepsilon_1+\varepsilon_2+\varepsilon_3}{1+2\varepsilon_1+\varepsilon_2}. \tag{14}$$

Recalling from Eq. (8) that the correlation width measure for a quantity f is defined as $\lambda_w^2(\tau)=|\Gamma_{f,f,2}(\tau)/\Gamma_{f,f,0}(\tau)|$ means that an estimate is needed for $\Gamma^{\text{upper}}_{\chi,\chi,0}(0)$. The choice for this depends on the initial condition applying to $\chi(\eta,0)$. In the case considered here where the starting phase is amorphous, i.e., $\chi(\eta,0)=0$, the sensible value for $\Gamma^{\text{upper}}_{\chi,\chi,0}(0)$ is $\Gamma_{\Psi,\Psi,0}(0)$, which reflects the fact that the kinetics are typically fast, and

so $\Gamma^{\text{upper}}_{\chi,\chi,0}(0)$ equilibrates with or follows the thermal initial condition $\Psi(\eta,0)$. Hence when $\Psi(\eta,0)=0$, then dividing Eq. (13) by $\Gamma_{\Psi,\Psi,0}(0)$ gives

$$\lambda^{\text{upper}}_{\chi,\chi}(\tau) = \sqrt{4\beta\tau + \lambda_{\Psi,\Psi}(0)^2}, \tag{15}$$

where $\lambda^{\text{upper}}_{\chi,\chi}(\tau)$ is the normalized upper correlation length of the crystalline fraction and $\lambda_{\Psi,\Psi}(\tau)$ is the normalized correlation length of the initial temperature profile. The actual correlation lengths (as opposed to the normalized form), denoted by $d^{\text{upper}}_{\chi,\chi}(t)$ and $d_{\Psi,\Psi}(t)$, are now obtained by substituting the scaling relationships from Sec. II D,

$$d^{\text{upper}}_{\chi,\chi}(t) = \sqrt{4\alpha\beta t + d_{T,T}(0)^2}, \tag{16}$$

where $\alpha=K_a/(\rho_o C_a)$ is the thermal diffusivity of the material.

Examining Eq. (16) that describes the upper bound estimator $d^{\text{upper}}_{\chi,\chi}(t)$ shows that up to a first order, the anisotropy in thermal parameters is associated with the thermal diffusivity of the medium through the ratio $\beta=(1+2\varepsilon_1+\varepsilon_2+\varepsilon_3)/(1+2\varepsilon_1+\varepsilon_2)$ irrespective of the shape of the initial temperature profile. Simplifying this ratio by neglecting the latent heat coefficient ε_2 due to its small value compared to the other coefficients yields

$$\beta \approx 1 + \frac{\varepsilon_3}{1+2\varepsilon_1}. \tag{17}$$

It is possible to apply sensitivity analysis on Eq. (17) to determine the significance of the anisotropies in thermal conductivity and specific heat on the overall thermal anisotropy of the system. Perturbing any of the coefficients ε by $\delta\varepsilon$ in Eq. (17) produces $\beta(\varepsilon+\delta\varepsilon)$, which upon expansion to first order yields

$$\beta(\varepsilon+\delta\varepsilon) \approx \beta(\varepsilon) + \frac{d\beta}{d\varepsilon}\delta\varepsilon. \tag{18}$$

The second term on the right-hand side represents the change in β due to variations in the coefficient ε. Normalizing the differential values of β and ε of the second term by their unperturbed values provides the sensitivity of β due to changes in any of the coefficients ε, denoted by S^{β}_{ε}, as

$$S^{\beta}_{\varepsilon} = \frac{\partial\beta}{\partial\varepsilon}\frac{\varepsilon}{\beta}, \tag{19}$$

where a zero sensitivity would indicate that changes in ε have no effect on β. Starting with the specific heat coefficient, ε_1, it can be shown that the sensitivity to this anisotropy term using Eq. (19) changes as $S^{\beta}_{\varepsilon_1}=0\rightarrow-\frac{1}{6}$ for all the permissible values of ε_1 and ε_2 as they change from $0\rightarrow1$. On the other hand, the sensitivity of β to changes in the thermal conductivity coefficient, ε_3, according to Eq. (19) has the values $S^{\beta}_{\varepsilon_3}=0\rightarrow\frac{1}{2}$ as ε_1 and ε_2 change from $0\rightarrow1$. Thus the sensitivity due to anisotropy in thermal conductivity $S^{\beta}_{\varepsilon_e}$ is larger than the anisotropy in specific heat, which means that changes in the thermal conductivity term ε_3 have the dominant effect on β and hence on the thermal diffusion process and length in the medium.

To proceed in the evaluation of the change in crystallization correlation length with time in Eq. (15) or (16), an initial temperature profile is needed. A typical thermal profile written using a laser or a probe will have a monotonically decreasing symmetric form that can be represented by a Gaussian function, and hence this will be employed for the initial temperature profile $\psi(\eta,0)$ with a length scale measure x_o. This function has a width parameter σ that describes the width of this distribution at $e^{-1/2}$ or 0.6 of its peak value. This function is written in normalized form as

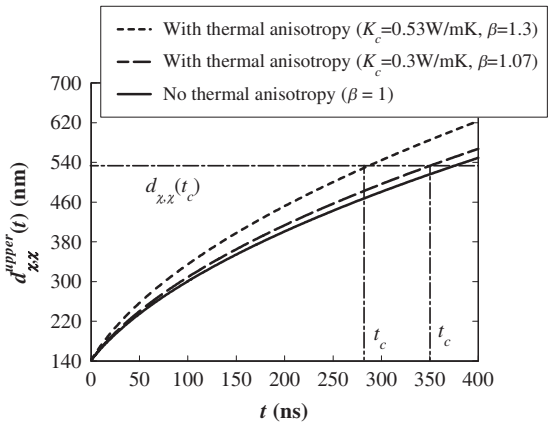

FIG. 1. Time evolution of the upper limit of the length of the crystallized region with and without the thermal anisotropies calculated using Eq. (16) and the material parameters for $Ge_2Sb_2Te_5$ listed in Table I.

$$\Psi(\eta,0) = \Psi_p e^{(-x_o^2/2\sigma^2)\eta^2}, \tag{20}$$

where $\Psi_p=(T_p-T_o)/T_o$, with T_p being the peak temperature. The peak temperature represents the magnitude of the energy density supplied by heat sources such as lasers or probes. Substituting Eq. (20) into Eq. (7) allows the evaluation of $\Gamma_{\Psi,\Psi,0}(0)$ and $\Gamma_{\Psi,\Psi,0}(0)$, which upon substitution into Eq. (8) yields the correlation width for the initial Gaussian temperature profile

$$\lambda_{\Psi,\Psi}(0)^2 = \frac{2\sigma^2}{x_o^2} \quad \text{or} \quad d_{T,T}(0)^2 = 2\sigma^2. \tag{21}$$

The evolution of $d^{\text{upper}}_{\chi,\chi}(t)$ with time can now be obtained by substituting Eq. (21) into Eq. (16). This is shown in Fig. 1 for an initial temperature pulse width $\sigma=100$ nm. The anisotropy coefficients and the thermal diffusivity are computed from the values in Table I. From the figure it can be seen that for the $Ge_2Sb_2Te_5$ parameters used in this work, the thermal anisotropies lead to a slight increase in $d^{\text{upper}}_{\chi,\chi}(t)$ with time compared with the isotropic case. Even with the large anisotropy in thermal conductivity (when using $K_c=0.53$ W/m K) this increase in $d^{\text{upper}}_{\chi,\chi}(t)$ is still modest. This has significant practical importance as the majority of modeling and simulation work on data storage applications employs the rather *ad hoc* assumption of isotropic thermal parameters. The above results indicate that such approximations have a wider validity than might have been expected. In particular they allow an isotropic kinetic analysis,[6] which brings in the dependence on parameters such as the annealing activation energy.

B. Upper estimate of the time at which phase change ceases

Reiterating, the upper bound estimator $d_{\chi,\chi}^{\text{upper}}(t)$ presented here derives from the heat flow equation and does not contain detailed information about the kinetics; i.e., Eq. (16) must be stopped at some time (t_c) when the phase-change process becomes insignificant. This happens when the initial temperature has fallen below the crystallization temperature T_c and phase change has ceased.

By exploring the properties of correlation moments it is possible to obtain an expression linking T_c and the correlation width $d_{\chi,\chi}(t_c)$ to estimate the width of the final crystallized region. The justification for the technique used relies on two factors, (i) Because the autocorrelation functions are integral measures their shape is relatively insensitive to the details of the temperature profile, and (ii) for conserved quantities, such as $\Psi(\eta,\tau)$, the autocorrelation moment $\Gamma_{\Psi,\Psi,0}(\tau)$ can be shown to be time independent[5] and scales as $\Psi_p(0)^2\lambda_{\Psi,\Psi}(0)^2$, where $\Psi_p(0)$ is the maximum temperature of the initial temperature profile. The latter property indicates that the autocorrelation moments for the temperature at times $\tau=0$ and $\tau=\tau_c$ approximately scale as

$$\frac{\Psi_c^2\lambda_{\chi,\chi}(\tau_c)^2}{\Psi_p(0)^2\lambda_{\Psi,\Psi}(0)^2}\approx 1, \tag{22}$$

with τ_c being the time at which Ψ_c occurs. Hence

$$\lambda_{\chi,\chi}(\tau_c)\approx\frac{\Psi_p(0)\lambda_{\Psi,\Psi}(0)}{\Psi_c}. \tag{23}$$

Substituting the values $d_{T,T}(0)=\sigma\sqrt{2}$ for an initial Gaussian profile with width $\sigma=100$ nm $T_c=446$ K from Table I and choosing $T_p=850$ K (above crystallization temperature T_c and below the melting temperature T_m and suitable for high crystallization rates[6]) yield $d_{\chi,\chi}(t_c)=533$ nm. Moreover, combining Eq. (23) with Eq. (15) it is possible to obtain an expression for the time τ_c where phase change ceases as

$$\tau_c=\frac{\lambda_{\Psi,\Psi}^2(0)}{4\beta}\left[\left(\frac{\Psi_p}{\Psi_c}\right)^2-1\right]. \tag{24}$$

For the material values listed in Table I and the same peak temperature, Eq. (24) yields a spreading cease time of $t_c=350$ ns. The calculated values of $d_{\chi,\chi}(t_c)$ and t_c for $Ge_2Sb_2Te_5$ are shown in Fig. 1 as the dash-dot lines, and it is interesting to note that the increase in thermal anisotropy (due to the increase in K_c) reduces the crystallization spreading time by approximately 70 ns, but at the same time increases the size of the crystalline mark.

With the exception of the anisotropy factor β in the denominator, it can be readily shown that Eq. (24) represents the time taken for the peak temperature in the initial Gaussian thermal profile to reduce to T_c and is thus a legitimate upper estimator for when thermal spreading stops to define the size of the crystalline mark. It can be observed that the thermal anisotropy term β in the correlation length in Eq. (16), after introducing the dimensional parameters in Eq. (24), is associated with the thermal diffusivity of the material. This suggests that the simpler isotropic heat diffusion equation can be used in thermal analysis, and that the effects of thermal anisotropies can be included by multiplying the thermal diffusivity by the anisotropy term β. This proposal is in need of further investigation.

IV. CONCLUSIONS

An analytical theory was presented in this work to identify the significance of thermal anisotropies on the amorphous-to-crystalline phase transition process. Correlation moment analysis produced a closed-form, time dependent upper estimator for the correlation length of the crystalline mark during cooling. This correlation length was mathematically in the form of a diffusion length with the anisotropy term $\beta\geq 1$ multiplied by the thermal diffusivity of the phase-change medium. This result could imply that the simpler isotropic thermal analysis can be extended to include anisotropic effects by multiplying the thermal diffusivity by the anisotropy factor. From published values of the thermal parameters of the phase-change material $Ge_2Sb_2Te_5$, it was found that the contribution of the thermal anisotropy to the heat diffusion process, and hence correlation length, is negligible. This outcome justifies ignoring anisotropies in analysis of thermal writing and reading in phase-change media, an assumption that is widely used. Sensitivity analysis on the anisotropy term β revealed that anisotropy in the thermal conductivity of the amorphous and crystalline phases has the significant effect on the heat diffusion process in the material, compared to the anisotropy in specific heat.

The correlation moment analysis was based on the heat diffusion process alone, and as a result produced analytical upper estimators of general nature for the correlation length and the time of when thermal, and hence phase-change spreading stops. The effect of the phase-change kinetics and the implications of using a delta function initial temperature profile are treated in detail elsewhere.

[1] C. Peng, L. Cheng, and M. Mansuripur, J. Appl. Phys. **82**, 4183 (1997).
[2] T. Ohta, K. Inoue, M. Uchida, K. Yoshioka, T. Akiyama, S. Furukawa, K. Nagata, and S. Nakamura, Jpn. J. Appl. Phys. **28**, 123 (1989).
[3] I. Friedrich, V. Weidenhof, W. Njoroge, P. Franz, and M. Wuttig, J. Appl. Phys. **87**, 4130 (2000).
[4] V. Weidenhof, I. Friedrich, S. Ziegler, and M. Wuttig, J. Appl. Phys. **89**, 3168 (2001).
[5] M. R. Belmont, J. Appl. Mech. **73**, 197 (2006).
[6] M. M. Aziz, M. R. Belmont, and C. D. Wright, "Ultra-Fast Heating and Resolution of Recorded Crystalline Marks in Phase-Change Media," J. Appl. Phys. (submitted).
[7] G. Zhou, Mater. Sci. Eng., A **304–306**, 73 (2001).
[8] H. C. F. Martens, R. Vlutters, and J. C. Prangsma, J. Appl. Phys. **95**, 3977 (2004).
[9] M. M. Aziz and C. D. Wright, J. Appl. Phys. **99**, 034301 (2006).
[10] P. K. Khulbe, E. M. Wright, and M. Mansuripur, J. Appl. Phys. **88**, 3926 (2000).
[11] H. E. Kissinger, Anal. Chem. **29**, 1702 (1957).
[12] T. Nonaka, G. Ohbayashi, Y. Toriumi, Y. Mori, and H. Hashimoto, Thin Solid Films **370**, 258 (2000).
[13] O. Bichet, C. D. Wright, Y. Samson, and S. Gidon, J. Appl. Phys. **95**, 2360 (2004).
[14] K. B. Blyuss, P. Ashwin, A. P. Bassom, and C. D. Wright, Phys. Rev. E **72**, 011607 (2005).
[15] J. Siegel, A. Schropp, J. Solis, C. N. Afonso, and M. Wuttig, Appl. Phys. Lett. **84**, 2250 (2004).
[16] J. Kalb, F. Spaepen, and M. Wuttig, J. Appl. Phys. **93**, 2389 (2003).
[17] N. Yamada, E. Ohno, K. Nishiuchi, and N. Akahira, J. Appl. Phys. **69**, 2849 (1991).

[18]T. Ohta and S. Ovshinsky, in *Photo-Induced Metastability in Amorphous Semiconductors*, edited by A. B. Kolobov (Wiley, Weinheim, 2003), Chap. 18.
[19]E. Kim, S. Kwun, S. Lee, H. Seo, and J. Yoon, Appl. Phys. Lett. **76**, 3864 (2000).
[20]V. Giraud, J. Cluzel, V. Sousa, A. Jacquot, A. Dauscher, B. Lenoir, H. Scherrer, and S. Romer, J. Appl. Phys. **98**, 013520 (2005).
[21]C. Peng and M. Mansuripur, Appl. Opt. **39**, 2347 (2000).
[22]S. Senkader and C. D. Wright, J. Appl. Phys. **95**, 504 (2004).
[23]A. Papoulis, *The Fourier Integral and its Applications* (McGraw-Hill, New York, 1987).
[24]M. M. Aziz and C. D. Wright, J. Appl. Phys. **97**, 103537 (2005).